Molecular Crystals and Liquid Crystals Science and Technology. Section A. Molecular Crystals and Liquid Crystals

Publication details, including instructions for authors and subscription information:
http://www.tandfonline.com/loi/gmcl19

Grandjean-Cano Texture under Weak Anchoring Conditions in Cholesteric Cells

M. Warenghem [a]

[a] Laboratoire de dynamique et structure des matériaux moléculaires, U.R.A. C.N.R.S. 801, Université des Sciences et Techniques de Lille, F 59655, VILLENEUVE D'ASCQ Cedex

Version of record first published: 24 Sep 2006.

To cite this article: M. Warenghem (1992): Grandjean-Cano Texture under Weak Anchoring Conditions in Cholesteric Cells, Molecular Crystals and Liquid Crystals Science and Technology. Section A. Molecular Crystals and Liquid Crystals, 220:1, 39-51

To link to this article: http://dx.doi.org/10.1080/10587259208033427

Mol. Cryst. Liq. Cryst., 1992, Vol. 220, pp. 39–51
Reprints available directly from the publisher
Photocopying permitted by license only

Printed in the United States of America

Grandjean-Cano Texture under Weak Anchoring Conditions in Cholesteric Cells†

M. WARENGHEM

Laboratoire de dynamique et structure des matériaux moléculaires, U.R.A. C.N.R.S. 801, Université des Sciences et Techniques de Lille, F 59655 VILLENEUVE D'ASCQ Cedex

(Received October 21, 1991; in final form January 16, 1992)

Structure of planar cholesteric cells under weak anchoring conditions has been considered from both theoretical and experimental point of view. Director distribution of the cell has been calculated in the frame of continuum theory, taking into account boundary conditions. Solutions are discussed with respect to anchoring energy, cell thickness and unperturbed cholesteric pitch. Considering a wedged cholesteric sample where planar weak anchoring is assumed at both interfaces, it is shown that two regimes exist: lined with Grandjean-Cano defects at high thicknesses and free of lines at low thicknesses. In such a wedge, the number of "missing" lines depends on anchoring energy, twist elastic constant and unperturbed cholesteric pitch. The position of the existing lines differs from that they have under strong anchoring conditions, the equidistance is lost. Experimental evidence of these two regimes is also reported.

Keywords: weak anchoring, Grandjean-Cano textures, cholesteric cells

INTRODUCTION

Any application involving liquid crystals requires the ability to properly align the material at the boundaries, usually glass plates; that is why many papers deal with this matter.[1] The orientation within a liquid crystal cell can theoretically be deduced from functional minimization of elastic energy with respect to a director distribution taking into account boundary conditions. Many geometries have been considered: thin or thick, plane parallel or wedged samples, free surface drop, etc. In most cases, strong anchoring prevails and the obtained director distribution gives a qualitative behavior of the cell which is usually sufficient. A more precise behavior has been obtained introducing weak anchoring boundary conditions but most of the papers deal with nematics, some with smectics.[2,3] In this paper, the influence of weak anchoring energy on Grandjean-Cano texture in a planar cholesteric cell is considered. This geometry and the associated defect structure, first observed by Grandjean,[4] has been extensively studied,[5–10] except the behavior of such cell under

† Presented at the 2nd International Topical Meeting on Optics of Liquid Crystals, Turin (1988).

less constraining boundary conditions. Also, the pitch value of twisted materials is derived from such a texture: the position of the lines in a wedged sample readily gives the pitch value, assuming strong boundary conditions.[11] The questions that will be answered in this paper are: does the position of the lines still remain under weak anchoring and is there any criterion to decide whether or not a given anchoring must be considered as strong or weak. The theoretical aspect is developed in the part A whereas the experimental evidence is reported in the part B.

A. THEORY

A-1) Notations–Equations

Let us consider a cholesteric contained in between two glass plates. These two plates are treated to lie down cholesteric molecules in the so called easy directions noted u_{01} and u_{02}, both contained in the glass planes. As a result, the twist axis is normal to the plates, parallel to the z-axis using the usual notation as depicted on the Figure 1. The lower plate contains the xy plane of the reference cartesian frame with the x-axis parallel to the easy direction u_{01}. The second plate, parallel to the other one is located at the spot height h (cell thickness) and for the sake of simplicity, the easy direction u_{02} is chosen parallel to the other one. In the simple model that is considered in this paper, the situation of a pure twist can reasonably be assumed, that means the director n coordinates reduce to:

$$n_x = \cos \Phi(z); \qquad n_y = \sin \Phi(z); \qquad n_z = 0 \tag{1}$$

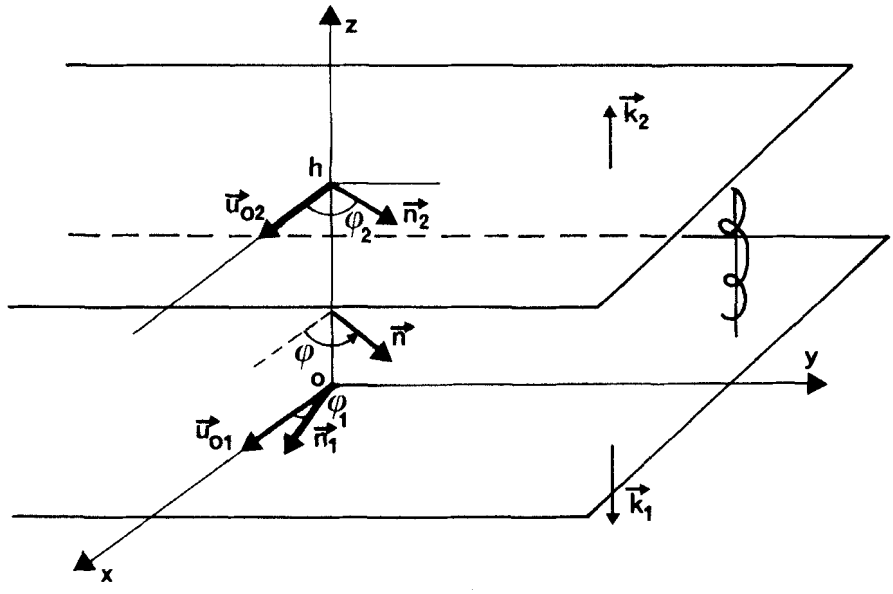

FIGURE 1 Geometry and notations.

Especially at the walls, director and angles are subscripted:

$$\begin{aligned} n_i &= n(\Phi_i), \qquad i = 1, 2 \\ \Phi_1 &= \Phi(z = 0), \qquad \Phi_2 = \Phi(z = h) \end{aligned} \tag{2}$$

In case of strong anchoring, both angles Φ_i reduce to zero.

The film structure can be deduced from continuum theory by minimizing the film energy F consisting of bulk energy F_b and surface energies F_{si}. We use the usual expressions for both contributions: their density are expressed as:

$$2.f_b = K_1.(\mathrm{div}n)^2 + K_2.(n.\mathrm{curl}n + q_0)^2 + K_3.(n \times \mathrm{curl}n)^2 \tag{3}$$

$$f_{si} = Y_{0i} - \Delta Y_i.(n_i.u_{0i})^2, \qquad i = 1, 2 \tag{4}$$

$$f = f_b + f_{s1} + f_{s2} \tag{5}$$

Expressions where K_i are the elastic constants of the cholesteric, q_0 the unperturbed cholesteric wave vector, Y_{0i} and ΔY_i are respectively the interfacial and anchoring energies at both interfaces of the cell.

Functional minimization of the energy 5 leads to a differential equations set, the solution of which gives the director distribution within the film. This set has been derived by Jenkins et al.[12] or under another form by De Gennes.[13] Using the pure twist situation, the splay and bend contributions do not intervene and the set write down:

$$K_2.n \times [\mathrm{grad}(q_0 - \Phi) \times n] = 0 \tag{6}$$

$$K_2.(n_i.\mathrm{curl}n_i + q_0).[(n_i.k_i)n_i - k_i] + n_i \times \frac{\partial F_{si}}{\partial n_j} = 0 \tag{7}$$

Where k_i is a unit vector normal to the walls and pointing out of the film. Using the notations introduced above, equilibrium equations 6 and 7 write down now:

$$\ddot{\Phi}_z = 0 \tag{8}$$

$$K.(q_0 - \dot{\Phi}_z) + \Delta Y_1.\sin(2.\Phi_1) = 0 \tag{9}$$

$$K.(q_0 - \dot{\Phi}_z) + \Delta Y_2.\sin(2.\Phi_2) = 0 \tag{10}$$

Where K stands for K_2.

Exact solution for this equation set comes through numerical processing, but to obtain some qualitative behavior, it is interesting to restrict the study to symmetrical films that is to say treatment at both interfaces is exactly the same. Therefore

anchoring energies are identical and using symmetry considerations one can assume equal anchoring angles:

$$\Delta Y_1 = \Delta Y_2 = \Delta Y \tag{11}$$

$$\Phi_1 = -\Phi_2 \tag{12}$$

Thus, the equations to be solved are written down:

$$\ddot{\Phi}_z = 0 \tag{13}$$

$$K.(q_0 - \dot{\Phi}_z) + \Delta Y.\sin(2.\Phi_1) = 0 \tag{14}$$

We now qualitatively discuss the solutions of these equations and give the associated cell structure.

A-2) Cell Structure

The bulk evolution for the twist angle $\Phi(z)$ is readily obtained from 13:

$$\Phi(z) = q.z + \Phi_1 \tag{15}$$

Where q is a constant, the actual wave vector of the bounded cholesteric. Its value depends on the cholesteric parameters (q_0, K), the boundary conditions (ΔY) and the cell thickness (h) and it is obtained from solution of Equation 14. The dependence of these different parameters on the wave vector following straight from the thickness dependence, we now focus on this point.

Starting from solution 15 applied to the upper wall, a first correlation between the wave vector and the thickness comes:

$$q.h = \Phi_2 - \Phi_1 \tag{16}$$

Using the symmetry 12 and inserting the relation 16 in 14, the wave vector q is thus solution of:

$$K.(q_0 - q) = \Delta Y.\sin(q.h) \tag{17}$$

This equation can be solved numerically and the curve $q = f(h)$ can be built up: The general trend is shown on the Figure 2. Let us try to understand the behavior of this curve.

First, the sin function ranging in between $(-1, +1)$, the wave vector is therefore limited between two values q_-, q_+:

$$q_- < q < q_+ \tag{18}$$

$$q_\pm = q_0 \pm \Delta Y/K \tag{19}$$

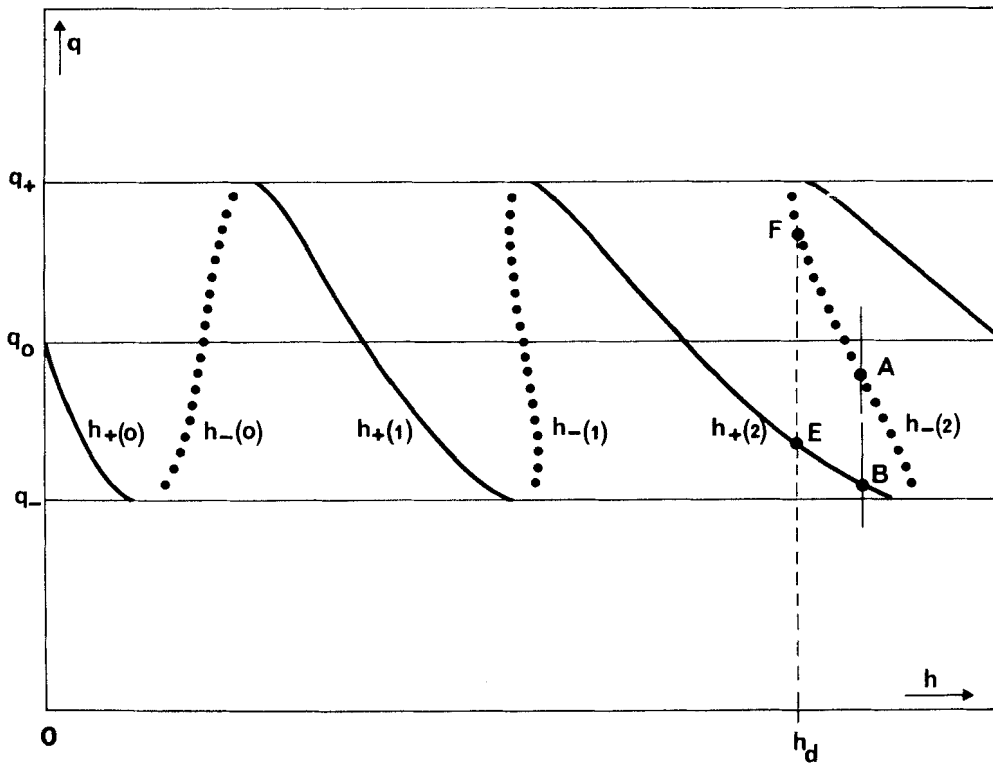

FIGURE 2 Wave vector versus thickness: computerized solution of Equation 17. Full lines represent the set noted h_+ in the text and dotted lines the set h_-.

For a given value of q, an infinity of values for the thickness h fulfill the relation 17. These values can be filed in two sets defined as follows:

$$\begin{aligned} h_+ &= h_+(q,k) = [\alpha + 2.k.\pi]/q; \\ h_- &= h_-(q,k) = [-\alpha + (2.k' + 1).\pi]/q \end{aligned} \tag{20}$$

k and k': integers

$$\alpha = \mathrm{ASN}[K.(q_0 - q)/\Delta Y] \tag{21}$$

These two sets are parts of the continuous curve $q = f(h)$ (see Figure 2) and are linked as follows:

$$\begin{aligned} h_+(q_-, k) &= h_-(q_-, k) \\ h_+(q_+, k) &= h_-(q_+, k - 1) \end{aligned} \tag{22}$$

Each branch intercepts the q_0 axis at thicknesses h_0 readily obtained from 17:

$$h_0 = k.p_0/2, \qquad k \text{ integer.} \tag{23}$$

Where p_0 is the unperturbed cholesteric pitch. More precisely, the even value for k are associated to the set h_+, whereas the odd values correspond to an interception of the set h_- with the q_0 axis.

As it can be seen on Figure 2, the function $q = f(h)$ is not monotonic. Especially for a large given thickness, it can have up to three values for q that fulfill the relation 17. The physical solution minimizes the energy of the film. According to the hypothesis (pure twist and symmetrical boundaries), this energy writes down:

$$f = K.(q_0 - q)^2/2 - 2.\Delta Y \cos^2(qh/2) \tag{24}$$

Obviously, closer to q_0 is q, smaller are both terms of this energy, therefore the physical solution is that corresponding to a q value the closest to q_0 (A preferred to B, Figure 2). Using this criterion, the actual value of the wave vector —i.e. the physical solution of 17— can be plotted, showing some discontinuities (Figure 3a). It is quite easy to issue the existence condition and the thickness position of these discontinuities.

First a discontinuity occurs as the derivative of a h_- curve calculated for q_0 is negative:

$$\left(\frac{dq}{dh_-}\right)_{q=q_0} < 0 \tag{25}$$

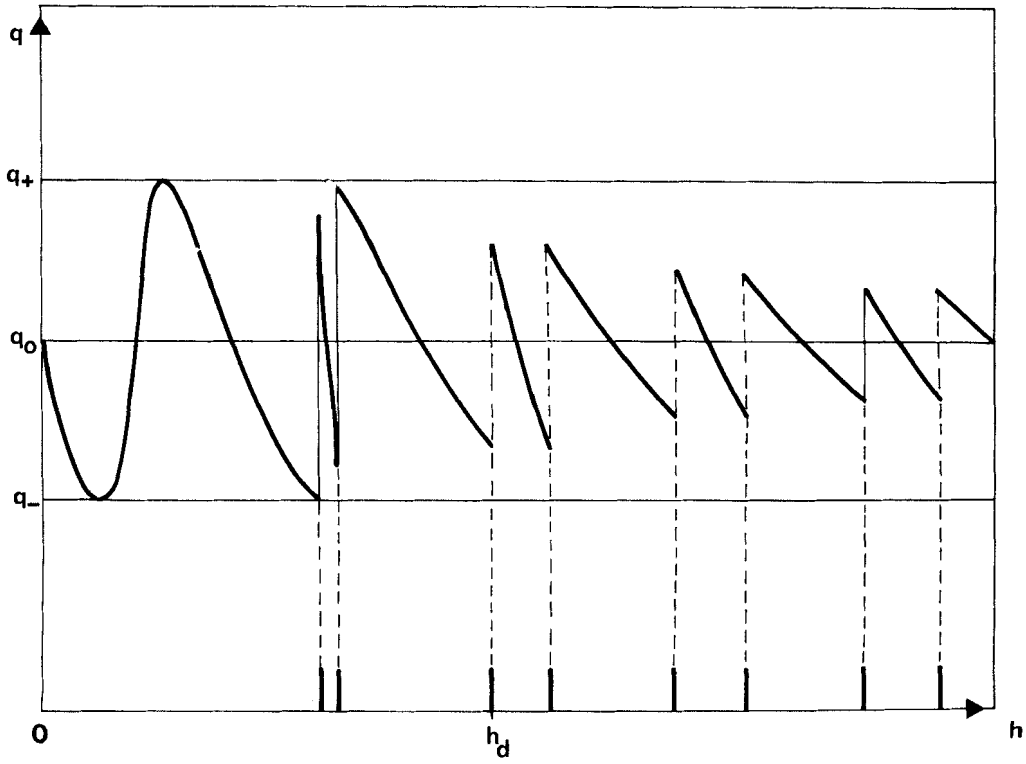

FIGURE 3 Wave vector versus thickness: (a) physical solution; (b) position of the Cano lines in the wedge.

This derivative can be calculated by differentiating Equation 17:

$$\frac{dq}{dh} = -\frac{q \cos qh}{\frac{K}{\Delta Y} + h \cos qh} \tag{26}$$

The interception of h_- with q_0 axis occurs for odd values of half unperturbed pitch p_0 (23) and therefore the wanted derivative is:

$$\left(\frac{dq}{dh}\right)_{q=q_0} = \frac{q_0}{\frac{K}{\Delta Y} - (2k + 1)\frac{p_0}{2}} \tag{27}$$

Thus applying condition 25, the existence of a discontinuity in the physical solution $q = f(h)$ is therefore given by:

$$K/\Delta Y < (2.k + 1).p_0/2 \tag{28}$$

The location h_d of a discontinuity on thickness abscissa is obtained in writing that for this thickness h_d, the two values of q mathematical solutions of 17 and belonging respectively to the set h_+ and h_- are symmetrical with respect to q_0 (E and F, Figure 2):

$$\begin{aligned} K\Delta q &= \Delta Y.\sin(q_0.h_d - \Delta q.h_d) \\ -K\Delta q &= \Delta Y.\sin(q_0.h_d + \Delta q.h_d) \\ \Delta q &= q_0 - q \end{aligned} \tag{29}$$

Yielding successively to:

$$\begin{aligned} 2.\Delta Y.\sin(q_0.h_d).\cos(\Delta q.h_d) &= 0 \\ = > \Delta q.h_d &= (2.m + 1).\pi/2, \qquad m \text{ integer} \end{aligned} \tag{30}$$

Finally the abscissa h_d are given by:

$$h_d.\cos(q_0.h_d) = (-1)^{m+1}.(2.m + 1).\frac{K}{\Delta Y}.\pi/2 \tag{31}$$

The discontinuity in the actual wave vector corresponds to a Grandjean-Cano line.[5] It is worth noting that in case of strong anchoring, $K/\Delta Y$ vanishes and the discontinuity abscissas become:

$$h_d = (2.m + 1).p_0/4 \tag{32}$$

That is exactly the Grandjean-Cano lines position under strong anchoring conditions as used in the pitch measurement. Here, we obtain both an existence condition (28) and the position (31) of the lines under any anchoring conditions.

A-3) Discussion

To discuss these two points, let us consider a wedged sample made of two identically treated glass plates. In case of strong anchoring, $K/\Delta Y$ vanishes and any positive integer value for k fulfills the relation 28: Cano lines are observed in the whole sample. In case of a weaker anchoring condition, $K/\Delta Y$ increases and the relation 28 is not fulfilled for first integer values. Let us assume that k_0 is the first integer that fulfills the existence condition (28): discontinuities occur starting from the k_0th curve of the set $h_{\pm}$. In other words, Cano lines do not exist at low thicknesses, k_0 lines are "missing." Contrary to strong anchoring where lines are equally spaced (a line is observed as thickness increases of half a pitch, starting from $p_0/4$), it can be seen on the Figure 3 that lines are paired, located on both sides of odd values of half pitch p_0, starting from $(2.k_0 + 1).p_0/2$. The distance between two paired lines can be small at first discontinuities, increases as thickness is larger and finally, at very large thicknesses, the lines are located at the same place as in case of strong anchoring. The exact position of the lines is given by relation 31 and it takes a numerical processing to go further, that is beyond the scope of this qualitative paper.

From these considerations, strong anchoring notion can be precised: an anchoring can be said strong as no lines are missing, in other words, as relation 28 is fulfilled for any integer. This yields to:

$$\Delta Y_{\text{strong}} > 2.K/p_0 \tag{33}$$

In case of weaker anchoring, a wedged sample experiences two orientational regimes: a free of lines regime at low thicknesses, and a lined regime at higher thicknesses, the lines being located as previously described. The limit between the two regions can be estimated from 28 for the first value of k ($k = 0$), giving something like a critical thickness:

$$h_c = K/\Delta Y \tag{34}$$

This is to be compared with the critical thickness introduced in hybrid nematic cell studies.[2] In such cells, competition occurs between surface torque and elastic bulk torque. At low thicknesses and strong anchoring energy, satisfying simultaneously easy directions at both interfaces would induce an enormous bulk distorsion energy: as a result the cell is homogeneous, one surface torque imposes its preferred orientation. At higher thicknesses, the cell is heterogeneous. A similar situation occurs in weakly anchored cholesteric cell where the best way to minimize the bulk distorsion at low thicknesses and low anchoring energies is to move the director away from the easy directions at interfaces, holding the twist as close as the natural one.

At thicknesses where first lines exist and are very close together (see first dis-

continuity on Figure 3b), the energy of each solutions of 17 hardly differs, both surfaces and bulk energy contributions are equivalent and the regime is unstable as experimentally observed and described in the next paragraph.

B) EXPERIMENTAL

The prominent feature of a planar cholesteric cell under weak anchoring conditions is the two possible regimes: lined or unlined. According to condition 28, at constant

TABLE I

Texture of the different studied samples. The concentration in cholesteryl pelargonate appears in the first column, followed by the pitch. The first line indicates how many times the glass has been rubbed. The number between parenthesis refers to the photographs

	Mixture ↓	$N \rightarrow 5$	10	20
1	80%, 0.15 μm	no lines no modulation	no lines no modulation	modulation
2	60%, 0.3 μm	modulation	modulation	lines
3	40%, 0.7 μm	modulation (1)	lines	lines
4	20%, 1.3 μm	modulation + lines (3)	lines	lines (2)

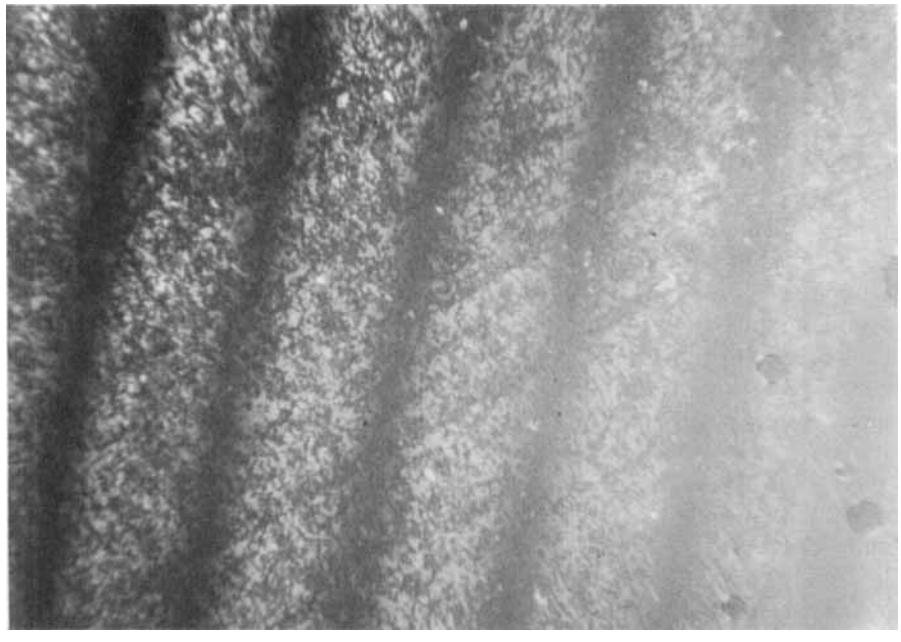

PHOTOGRAPH 1 Mixture of 40% cholesteryl pelargonate, 60% nematic observed through polarizing microscope with polarizers slightly uncrossed (≈2°, ×10), glass plates rubbed 5 times. Pitch of the mixture: 0.7 μm. See Color Plate I.

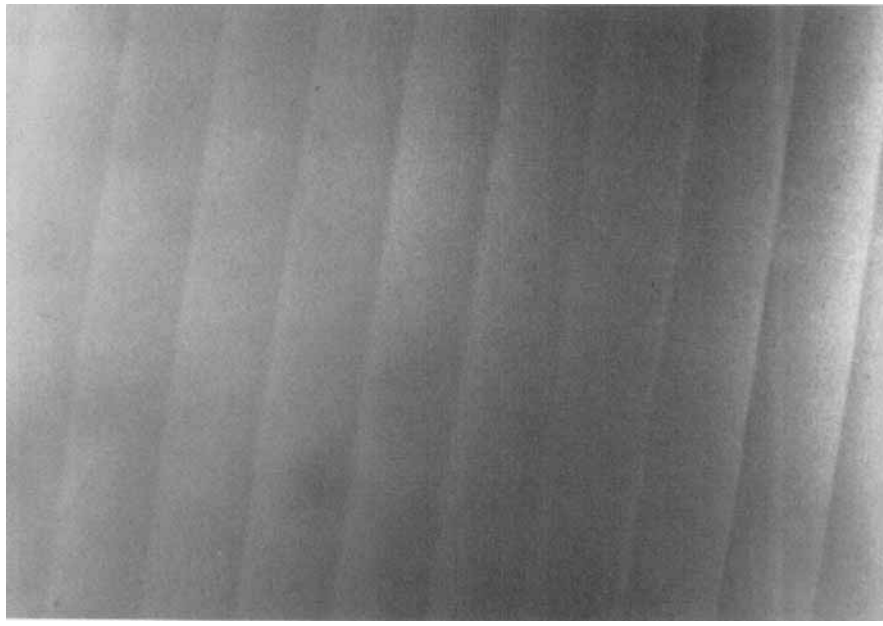

PHOTOGRAPH 2 Mixture of 20% cholesteryl pelargonate, 80% nematic observed through polarizing microscope with polarizers slightly uncrossed (≈10°, ×10), glass plates rubbed 20 times. Pitch of the mixture: 1.3 μm. See Color Plate II.

unperturbed pitch, lines disappear as the anchoring is weaker, reversely at constant anchoring conditions, lines disappear as the pitch is decreased (supposing that the twist constants do not vary). We present here experimental results where these two features have been observed. Several wedged samples where anchoring conditions have been varied and filled with cholesteric material having different pitches have been studied.

Wedged samples have been prepared using glass plates preliminarly cleaned and different spacers that insure a wedge angle adapted for the lines to be observable comfortably using low power microscope objective (×10, ×20).

Different anchoring energies have been obtained by rubbing the glasses under the same pressure back and forth n times using diamond paste (0.25 μm grain size). Only three cases are herein reported (n = 5, 10, 20) although others have been studied: n = 2 gives a so weak anchoring that no correct alignment has been obtained contrary to the case n = 50 giving a very strong anchoring. The three reported cases look the best to observe the critical region theoretically deduced in this paper. Obviously these values stand for the used mixtures: the critical region being related not only to anchoring energies but also to physical characteristics of the cholesteric, twist constant and pitch.

The basic cholesteric material used is the cholesteryl pelargonate. The pitch has been varied by mixing the pelargonate with an eutectic nematic mixture (ZLI 1083, Merck). The mixture has been introduced in the wedge by capillarity at a temperature high enough for the mixture to be isotropic and then the sample is slowly cooled down to a temperature around 35°C: the mixture is in the cholesteric phase.

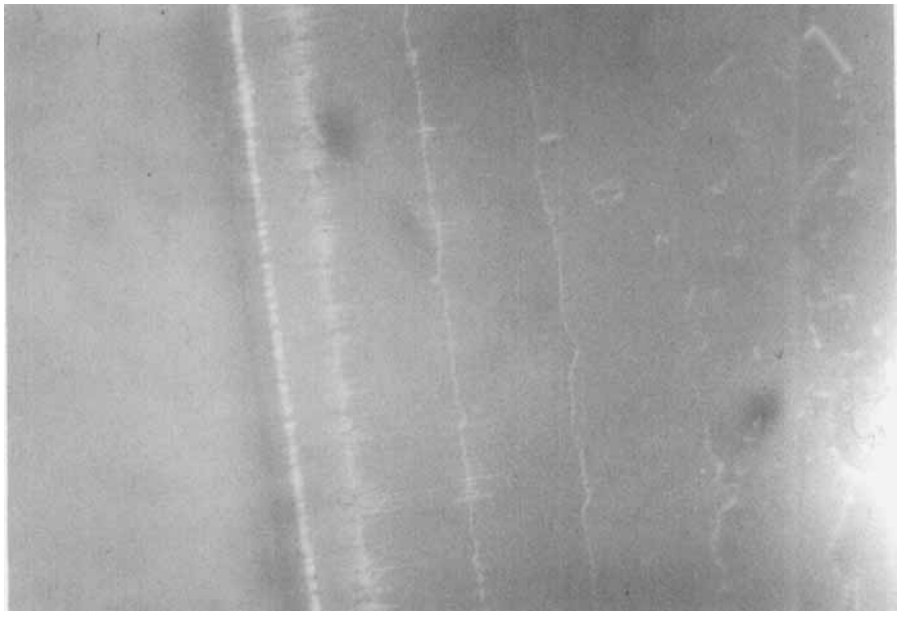

$\rightarrow h$

PHOTOGRAPH 3 Same as Photograph 2, but glass plates rubbed only 5 times. Large white line corresponds to thickness zero. See Color Plate III.

Four mixtures have been studied: 80%, 60%, 40% and 20% concentration of cholesteryl pelargonate in the nematic compound, they are referred respectively as mixture 1, 2, 3, 4.

The samples, placed in an oven (METTLER), have been observed through a polarizing microscope with low powers objectives ($\times 10$, $\times 20$), between crossed or slightly uncrossed (few degrees), in a position of the revolving table that improves the visibility of the lines. When no lines exist, a linearly polarized light experiences a rotation θ of its polarization direction according to De Vries[14]:

$$\theta = -\frac{\pi}{4}\frac{\Delta n^2}{\lambda^2}\frac{p}{1-\dfrac{\lambda^2}{n^2 p^2}}h \tag{35}$$

As the thickness increases, the q wave vector continuously oscillates between the two values $q_\pm$ (19), therefore the rotation θ oscillates as well: as a result the sample observed between crossed polarizers shows a modulation of the emerging light. The amplitide of this modulation depends on the anchoring energy (see 19), it vanishes as:

$$\frac{\Delta Y}{K} \ll q_0 \equiv \frac{p_0 . \Delta Y}{K} \ll 2\pi \tag{36}$$

The different observations are presented in the Table I and three of these are shown on Photographs 1, 2, 3. For the mixture 1, lines have been observed only for glass plates rubbed 50 times. Modulation has been observed for weak anchoring energies ($n = 20$), but for $n = 5$, 10 anchoring must be weak enough for the condition 36 to be fulfilled and no modulation has been observed. For mixture 2, a lined structure has been observed with $n = 20$ and modulation in the two other cases. For mixture 3, lines have been observed in both cases $n = 10$ and $n = 20$; modulation has been observed at $n = 5$; this is shown on Photograph 1. For mixture 4, lined structure has been observed for $n = 10$ and 20, shown on Photograph 2. On the Photograph 3, corresponding to a weak anchoring energy $n = 5$ it can be seen a lined structure at high thicknesses and a "first" line very diffuse: this corresponds to two lines close together in a region where surface energies and bulk energy are equivalent and different mathematical solutions are physically equivalent.

On the Table I, the main feature deduced from theory can be noted: at constant pitch value, lined structure appears with high anchoring energy; at constant anchoring energy, lined structure appears with high pitch value.

CONCLUSION

In this paper, the orientational structure of a planar cholesteric wedged cell has been investigated considering different thicknesses and anchoring energies. By minimizing the total free energy of the film, taking into account boundary conditions, two regimes have been obtained for the cell: with and without Cano defects. Under strong anchoring conditions, Cano lines exist as the thickness increases by one unperturbed cholesteric pitch. This well known situation is used to measure the pitch itself. What is new is the behavior of the cell as the surface strength releases: the Cano lines no longer exist at low thicknesses, totally disappearing under very weak anchoring conditions. Also, the position of the lines can be different from that observed under strong anchoring, therefore in any pitch measurement, it must be ensured that strong anchoring is effectively fulfilled: no missing lines at low thicknesses and equidistance of the lines are the right criterion. Finally, a more precise model should involve the lines energy as calculated by G. Malet.[15] Also a further study should be undertaken that takes into account the Kleman model.[16] Actually, as described by Bouligand,[17] the planar model[7] stands for the first line whereas the Kleman model stands for the next. Another question has to be considered: there are simple and double lines,[10] do their existence linked with anchoring strengths?

References

1. J. Cognard, *Mol. Cryst. Liq. Cryst. Suppl. 1*, **78**, (1982).
2. G. Barbero, N. V. Madhusudana and G. Durand, *J. de Phys. Lett.*, **45**, L613 (1984).
3. M. Warenghem and N. Isaert, *J. of Optics*, **16**, 1, 37 (1985).
4. F. Grandjean, *C.R.A.S.*, **172**, 71 (1921).

5. G. Friedel, *Ann. Phys.*, **18**, 273 (1922).
6. R. Cano, *Bull. Soc. Fr. Minera. Cristallo.*, **90**, 333 (1967); **91**, 20 (1968).
7. P. G. De Gennes, *C.R.A.S.*, **B266**, 571 (1968).
8. P. Chatelain and M. Brunet-Germain, *C.R.A.S.*, **268**, 1010 (1969).
9. Orsay Liquid Crystal Group, *Phys. Lett.*, **28A**, 687 (1969).
10. P. Malet and J. C. Martin, *Jour. de Phys.*, **40**, 355 (1979).
11. N. Isaert, G. Joly, C. Destrade and N.-H. Tinh, *Rev. Phys. Appl.*, **23**, 273 (1988).
12. J. T. Jenkins and P. J. Barat, *Quat. J. Mech. Appl. Math.*, **27**, 111 (1974).
13. P. G. De Gennes, The physics of liq. cryst., Clarendon, Oxford, 68, (1974).
14. H. L. De Vries, *Acta Cryst.*, **4**, 219 (1951).
15. G. Malet, J. Marignan and O. Parodi, *J. de Phys.*, **37**, 865 (1976).
16. M. Kleman and J. Friedel, *J. de Phys. Coll.*, **30**, C4-43 (1969).
17. Y. Bouligand, *J. de Phys.*, **35**, 959 (1974).